Full-Duplex Enabled Integrating Communication and Computation: Joint Beamforming and Power Optimization With Imperfect CSI

Hualiang Luo, Quanzhong Li, Qi Zhang, and Yiqing Li

***Abstract*— This letter investigates a full-duplex enabled network that integrates communication and over-the-air computation (AirComp), where the base station (BS) performs uplink process for AirComp and downlink process for communication over the same time-frequency resources. Consider the case of imperfect channel state information, we formulate a stochastic sum rate maximization problem such that the mean square error of AirComp should be less than a given threshold and each node's power budget is limited. To solve the stochastic optimization problem, we propose a fast stochastic algorithm which jointly optimizes the beamforming at the BS and the power factors of sensors, and the solution of each optimization variable has a closed or semi-closed form. The numerical results show the effectiveness of the proposed algorithm.**

***Index Terms*— Over-the-air computation (AirComp), full-duplex communication, stochastic optimization, robust resource allocation, beamforming.**

I. Introduction

With the explosive growth in the number of IoT devices [1], the communication overhead between mobile devices and the base station (BS) that collects the data becomes dominant. However, the extensive data transmission among the BS and sensors may exacerbate a severe communication bottleneck. It is important to develop an efficient scheme to aggregate the massive distributed data, and over-the-air computation (AirComp) is a promising technology that utilizes the signal-superposition property of a multiple access channel for efficient functional data aggregation (such as arithmetic mean, weighted sum, geometric mean, Euclidean norm, polynomial, and other nomographic functions) [2], [3].

Although the AirComp technology has such advantages, it cannot completely replace the traditional information communication. Besides, the available spectrum resource is limited, and it is predictable that the spectrum competition between the existing wireless network and the AirComp network will tend to intensify. To alleviate this competition, researchers intended to integrate both technologies. The authors in [3] studied a wireless network with AirComp in the uplink and broadcast in the downlink. In [4], a superposition coded transmit signal was constructed to realize the functionalities of target sensing, intelligent computing, and information communication over the same spectrum. Besides, the authors in [5] proposed two network frameworks that utilize dual-function radar communication to achieve target sensing and AirComp. In [6], the authors developed a framework that integrated AirComp and wireless power transfer in time division manner.

In addition, full-duplex is also a common technology for integrating dual function over the same time-frequency resources, such as integrating wireless power transfer and mobile edge computing [7], integrating target sensing and communication [8], integrating device-to-device communication and wireless power transfer [9], and integrating AirComp and artificial noise transfer [10].

Based on the above observations and motivated by the great success of full-duplex technology in wireless communications, we aim to leverage full-duplex technology for the integration of multiple different devices engaged in over-the-air computation or communication within a network sharing the same time-frequency resources. To the best of our knowledge, there is no investigation on the full-duplex enabled integrating AirComp and communication. In this letter, we consider that in a wireless network, a multi-antenna full-duplex BS serves as a fusion center for L single-antenna sensors and a base station for downlink communication of K users.

The main contributions of this letter are summarized as follows:

- We consider a full-duplex enabled wireless network that integrates AirComp and communication, where a multi-antenna full-duplex BS simultaneously operates AirComp for sensors and communication for users, over the same time-frequency resources. Table I provides a comparison of the proposed scheme with the typical works.
- In the case of imperfect channel state information (CSI), we construct a stochastic sum rate maximization problem subject to an mean-squared error (MSE) threshold of sensors' data aggregation and the power budget of each node. To solve the stochastic optimization problem, we propose a fast stochastic algorithm combining alternating optimization and consensus alternating direction method of multipliers (consensus-ADMM). In the proposed algorithm, a new surrogate function has been constructed to avoid semidefinite relaxation (SDR) to achieve lower computation complexity, and the closed (or semi-closed) form solution of each optimization variable has been derived.

Manuscript received 16 April 2024; accepted 12 May 2024. Date of publication 16 May 2024; date of current version 12 July 2024. This work was supported in part by the National Natural Science Foundation of China under Grant 62272493 and Grant 62102096, in part by the Guangdong Basic and Applied Basic Research Foundation under Grant 2023A1515011201 and Grant 2024A1515011823, and in part by the Guangzhou Basic and Applied Basic Research Foundation under Grant 2024A04J4297. The associate editor coordinating the review of this letter and approving it for publication was G. Thadeu Freitas de Abreu. *(Corresponding author: Quanzhong Li.)*

Hualiang Luo and Qi Zhang are with the School of Electronics and Information Technology, Sun Yat-sen University, Guangzhou 510006, China (e-mail: luohliang@mail2.sysu.edu.cn; zhqi26@mail.sysu.edu.cn).

Quanzhong Li is with the School of Computer Science and Engineering, Sun Yat-sen University, Guangzhou 510006, China (e-mail: liquanzh@mail.sysu.edu.cn).

Yiqing Li is with the School of Computer Science and Technology, Guangdong University of Technology, Guangzhou 510006, China (e-mail: liyiq5@gdut.edu.cn).

Digital Object Identifier 10.1109/LCOMM.2024.3401687

TABLE I
THE COMPARISON OF THE PROPOSED SCHEME WITH THE TYPICAL WORKS

Integration Mode	Time	Spectrum	network type	communication model	CSI model
two-way relay [3]	✓	✓	Homegeneous	broadcast	bounded uncertainty
multi-objective optimization [4]	✓	✓	Homegeneous	info. commun.	perfect
dual-functional technique [5]	✓	✓	Homegeneous	null	perfect
time division [6]		✓	Homegeneous	null	perfect
full-duplex (this paper)	✓	✓	Heterogeneous	info. commun.	stochastic uncertainty

The abbreviation of "info. commun." denotes information communication.

- Numerical results demonstrate the superiority of our proposed algorithm compared to the existing scheme, in terms of sum rate and computation complexity.

II. System Model

Considering a network consisting of a full-duplex BS equipped with N_b transmit antennas and N_b receive antennas, L sensors equipped with single-antenna, and K wireless users equipped with single-antenna. The BS aggregates the sensing signals received from all sensors and simultaneously transmits the communication signals to the users. Denote s_l as the pre-processing data of the l-th sensor and x_k as the BS transmits the communication signal to the k-th user, where s_l and x_k are assumed to be circularly symmetric complex Gaussian with zero mean and covariance $\mathbb{E}[s_l s_l^\dagger] = \mathbb{E}[x_k x_k^\dagger] = 1$, $\mathbb{E}[s_l s_{l'}^\dagger] = \mathbb{E}[x_k x_{k'}^\dagger] = 0, l = 1, \ldots, L, k = 1, \ldots, K, l \neq l', k \neq k'$ [3].

Denote the channel from the l-th sensor to the BS as $\mathbf{g}_l \in \mathbb{C}^{N_b \times 1}$, the channel from the BS to the k-th user as $\mathbf{h}_k \in \mathbb{C}^{N_b \times 1}$, and the effective self-interference channel of the BS as $\mathbf{J} \in \mathbb{C}^{N_b \times N_b}$. Consider the uncertainties of the CSI and model them as [12]

$$\mathbf{g}_l = \bar{\mathbf{g}}_l + \Delta\mathbf{g}_l,\ \mathbf{h}_k = \bar{\mathbf{h}}_k + \Delta\mathbf{h}_k,\ \mathbf{J} = \sqrt{\alpha}(\bar{\mathbf{J}} + \Delta\mathbf{J}), \tag{1a}$$

$$\Delta\mathbf{g}_l = \mathbf{\Theta}_{g,l}^{\frac{1}{2}}\tilde{\mathbf{g}}_l,\ \Delta\mathbf{h}_k = \mathbf{\Theta}_{h,k}^{\frac{1}{2}}\tilde{\mathbf{h}}_k,\ \Delta\mathbf{J} = \mathbf{\Theta}_J^{\frac{1}{2}}\tilde{\mathbf{J}}\mathbf{\Psi}_J^{\frac{1}{2}}, \tag{1b}$$

where $\bar{\mathbf{g}}_l$, $\bar{\mathbf{h}}_k$ and $\bar{\mathbf{J}}$ are the estimated CSI, $\Delta\mathbf{g}_l$, $\Delta\mathbf{h}_k$ and $\Delta\mathbf{J}$ are the channel estimation errors, $\tilde{\mathbf{g}}_l$, $\tilde{\mathbf{h}}_k$ and $\tilde{\mathbf{J}}$ are independent and identically distributed (i.i.d.) Gaussian random variables with zero mean and unit variance, the row covariance matrices for the channel estimation errors are denoted by $\mathbf{\Theta}_{g,l}$, $\mathbf{\Theta}_{h,k}$ and $\mathbf{\Theta}_J$ while $\mathbf{\Psi}_J$ represents the column covariance matrix of $\Delta\mathbf{J}$, and α models the effect of passive loop-interference suppression such as antenna isolation [10].

Thus, the received signals at the BS and the k-th user can be expressed as

$$\mathbf{y}_b = \sum_{l=1}^{L} \mathbf{g}_l a_l s_l + \mathbf{J}\sum_{k=1}^{K} \mathbf{w}_k x_k + \mathbf{n}_b, \tag{2}$$

$$y_k = \mathbf{h}_k^\dagger \sum_{k'=1}^{K} \mathbf{w}_{k'} x_{k'} + n_k, \tag{3}$$

where $a_l \in \mathbb{C}$ is the power factor of the l-th sensor, $\mathbf{w}_k \in \mathbb{C}^{N_b \times 1}$ is the BS beamforming vector for the k-th user, $\mathbf{n}_b \in \mathcal{CN}(\mathbf{0}, \sigma^2\mathbf{I})$ and $n_k \in \mathcal{CN}(0, \sigma_k^2)$ are the noise at the BS and the k-th user, respectively.

By multiplying an aggregation vector $\mathbf{u} \in \mathbb{C}^{N_b \times 1}$, the signal recovered by the BS is given by

$$\hat{s} = \mathbf{u}^\dagger \mathbf{y}_b. \tag{4}$$

Considering the sum operation as the aggregation function, i.e., $s = \sum_{l=1}^{L} s_l$ [3], [4]. To quantify the AirComp performance, the MSE is used to measure the distortion of the data aggregation result. Define $\mathbf{w} = \left[\mathbf{w}_1^T, \ldots, \mathbf{w}_K^T\right]^T$, $\mathbf{a} = [a_1, \ldots, a_K]^T$, and the MSE at the BS is given as follow

$$\begin{aligned}\mathrm{MSE}(\mathbf{u}, \mathbf{a}, \mathbf{w}) = \|s - \hat{s}\|^2 = \sum_{l=1}^{L} \left\|\mathbf{u}^\dagger \mathbf{g}_l a_l - 1\right\|^2 \\ + \sum_{k=1}^{K} \left\|\mathbf{u}^\dagger \mathbf{J} \mathbf{w}_k\right\|^2 + \sigma^2 \|\mathbf{u}\|^2.\end{aligned} \tag{5}$$

The signal-to-interference-to-noise ratio (SINR) is commonly employed to evaluate the quality of service of communication. The interference for the k-th user comes from the intra-system interference due to signals transmitted to other users and the inter-system interference from sensors. When the number of sensors is large and the sensors are far from the users, the interference caused by the sensors to the k-th user approaches to be Gaussian [11]. Thus, the SINR at k-th user can be expressed as

$$\gamma_k = \frac{\mathbf{w}_k^\dagger \mathbf{h}_k \mathbf{h}_k^\dagger \mathbf{w}_k}{\sum_{k'=1, k' \neq k}^{K} \mathbf{w}_{k'}^\dagger \mathbf{h}_k \mathbf{h}_k^\dagger \mathbf{w}_{k'} + \sigma_k^2}, \tag{6}$$

where σ_k^2 contains the noise and the interference caused by the sensors at k-th user. Incidentally, if the BS is far from sensors or users, one may consider employing relay [9] or reconfigurable intelligent surface [13], [14] for assistance.

Based on (6), the sum rate of users can be expressed as $\sum_{k=1}^{K} \log(1 + \gamma_k)$. Specifically, we consider the following stochastic sum rate maximization problem

$$\max_{\mathbf{u}, \mathbf{a}, \mathbf{w}} \quad \mathbb{E}\left[\sum_{k=1}^{K} \log(1 + \gamma_k)\right] \tag{7a}$$

$$\text{s.t.} \quad \mathbb{E}\left[\mathrm{MSE}(\mathbf{u}, \mathbf{a}, \mathbf{w})\right] \leq \xi, \tag{7b}$$

$$\|\mathbf{w}\|^2 \leq P_{\mathrm{BS}}, \tag{7c}$$

$$|a_l|^2 \leq P_l,\ l = 1, \ldots, L, \tag{7d}$$

where constraint (7b) ensures that the MSE at the BS remains below a given threshold ξ, constraints (7c) and (7d) limit the transmission power of the BS and sensors, P_{BS} and P_l are the power budget of BS and the l-th sensor, respectively.

III. Proposed Algorithm

In this section, we propose a fast stochastic algorithm to solve the stochastic optimization problem (7). Due to the coupling optimization variables in problem (7), we optimize the variables alternatively [13], [14].

A. Optimize $\mathbf{u}$ and $\mathbf{a}$

Optimize $\mathbf{u}$ and $\mathbf{a}$ when $\mathbf{w}$ is given. Since the optimization variables $\mathbf{u}$ and $\mathbf{a}$ only appear in the constraints of problem (7),

the problem is transformed into an MSE minimization problem to expand the feasible region of $\mathbf{w}$ as much as possible. Thus, problem (7) is rewritten as

$$\min_{\mathbf{u},\mathbf{a}} \quad \mathbb{E}\left[\mathrm{MSE}(\mathbf{u},\mathbf{a},\mathbf{w})\right] \tag{8a}$$

$$\text{s.t.} \quad |a_l|^2 \le P_l,\ l=1,\ldots,L. \tag{8b}$$

Because the optimization variables $\mathbf{u}$ and $\mathbf{a}$ are still coupling in problem (8), we optimize them alternatively.

Before optimizing each variable, we convert the constraint (7b) into a more traceable form. As in [12], the MSE expectation can be expressed as the following equation

$$\begin{aligned}\mathbb{E}\left[\mathrm{MSE}(\mathbf{u},\mathbf{a},\mathbf{w})\right] &= \sigma^2\mathbf{u}^\dagger\mathbf{u} + L \\ &+ \textstyle\sum_{l=1}^{L}\left(|a_l|^2\mathbf{u}^\dagger(\boldsymbol{\Theta}_{g,l}+\bar{\mathbf{g}}_l\bar{\mathbf{g}}_l^\dagger)\mathbf{u} - 2\Re\left\{\mathbf{u}^\dagger\bar{\mathbf{g}}_l a_l\right\}\right) \\ &+ \textstyle\sum_{k=1}^{K}\alpha\mathbf{u}^\dagger\left(\mathrm{tr}(\mathbf{w}_k\mathbf{w}_k^\dagger\boldsymbol{\Psi}_J)\boldsymbol{\Theta}_J + \bar{\mathbf{J}}\mathbf{w}_k\mathbf{w}_k^\dagger\bar{\mathbf{J}}^\dagger\right)\mathbf{u}.\end{aligned} \tag{9}$$

1) Optimize $\mathbf{u}$ *When* $\mathbf{a}$ *and* $\mathbf{w}$ *Are Given:* Problem (8) is recast as

$$\min_{\mathbf{u}} \ \mathbb{E}\left[\mathrm{MSE}(\mathbf{u},\mathbf{a},\mathbf{w})\right]. \tag{10}$$

As an unconstrained convex problem, we can obtain a closed-form solution for problem (10) by setting the first-order derivative to zero, which is

$$\begin{aligned}\mathbf{u} = &\left(\textstyle\sum_{k=1}^{K}\alpha(\mathrm{tr}(\mathbf{w}_k\mathbf{w}_k^\dagger\boldsymbol{\Psi}_J)\boldsymbol{\Theta}_J + \bar{\mathbf{J}}\mathbf{w}_k\mathbf{w}_k^\dagger\bar{\mathbf{J}}^\dagger)\right. \\ &\left.+\textstyle\sum_{l=1}^{L}(|a_l|^2(\boldsymbol{\Theta}_{g,l}+\bar{\mathbf{g}}_l\bar{\mathbf{g}}_l^\dagger)) + \sigma^2\mathbf{I}\right)^{-1}\left(\textstyle\sum_{l=1}^{L}\bar{\mathbf{g}}_l a_l\right).\end{aligned} \tag{11}$$

2) Optimize $\mathbf{a}$ *When* $\mathbf{u}$ *and* $\mathbf{w}$ *Are Given:* Problem (8) is recast as

$$\min_{\mathbf{a}} \quad \mathbb{E}\left[\mathrm{MSE}(\mathbf{u},\mathbf{a},\mathbf{w})\right] \tag{12a}$$

$$\text{s.t.} \quad |a_l|^2 \le P_l,\ l=1,\ldots,L. \tag{12b}$$

Since the elements in $\mathbf{a}$ are not coupled with each other, they can be solved in parallel. Take the l-th element in $\mathbf{a}$ as an example, and the corresponding optimization problem is

$$\min_{a_l} \quad |a_l|^2\mathbf{u}^\dagger(\boldsymbol{\Theta}_{g,l}+\bar{\mathbf{g}}_l\bar{\mathbf{g}}_l^\dagger)\mathbf{u} - 2\Re\left\{\mathbf{u}^\dagger\bar{\mathbf{g}}_l a_l\right\} \tag{13a}$$

$$\text{s.t.} \quad |a_l|^2 \le P_l. \tag{13b}$$

Problem (13) is a convex quadratically constrained quadratic problem (QCQP) with one constraint, and the solution is given as [15]

$$a_l = (\mathbf{u}^\dagger(\boldsymbol{\Theta}_{g,l}+\bar{\mathbf{g}}_l\bar{\mathbf{g}}_l^\dagger)\mathbf{u} + \mu_l)\bar{\mathbf{g}}_l^\dagger\mathbf{u}, \tag{14}$$

where $\mu_l \ge 0$ is the dual variable that can be obtained by bisection method [15].

Note that problems (10) and (12) are always feasible. If the optimized MSE is less than the specified threshold ξ, problem (7) is feasible; otherwise, problem is infeasible with the currently given $\mathbf{w}$.

B. Optimize $\mathbf{w}$

Optimize $\mathbf{w}$ when $\mathbf{u}$ and $\mathbf{a}$ are given, and problem (7) is transformed into

$$\max_{\mathbf{w}} \quad \textstyle\sum_{k=1}^{K}\mathbb{E}\left[\log\left(1+\gamma_k\right)\right] \tag{15a}$$

$$\text{s.t.} \quad \mathbb{E}\left[\mathrm{MSE}(\mathbf{u},\mathbf{a},\mathbf{w})\right] \le \xi, \tag{15b}$$

$$\|\mathbf{w}\|^2 \le P_{\mathrm{BS}}. \tag{15c}$$

Due to the fractions in γ_k and logarithmic functions in (15a), it is hard to obtain the closed-form expression of the sum rate of users. Therefore, we propose a fast stochastic algorithm to solve problem (15). Different from the constrained stochastic successive convex approximation (CSSCA) [16] which applies SDR and solves a series of semidefinite programmings (SDPs), we construct a new surrogate function which does not rely on semidefinite relaxation, and only a series of QCQPs need to be solved in the proposed fast stochastic algorithm. Employing consensus-ADMM [15] to solve the QCQPs, which has lower computational complexity than solving SDPs by the interior point method. In addition, the solution obtained by the proposed algorithm is already rank-one, which also avoids the performance loss caused by recovering a rank-one solution from the high-rank solution obtained by solving an SDP.

In $(t+1)$-th iteration, the surrogate function of the objective function (15a) is given as follow

$$\begin{aligned}g(\mathbf{w};\mathbf{w}^t) = &\textstyle\sum_{k=1}^{K}\left((1-\rho^t)\,f_k^t\right. \\ &+\rho^t\left(-\log(\mathbf{w}^{t\dagger}\mathbf{H}_{u,k}^t\mathbf{w}^t+\sigma_k^2)\right. \\ &\left.\left.+\log(\mathbf{w}^{t\dagger}\mathbf{H}_{u/k}^t\mathbf{w}^t+\sigma_k^2)\right)\right. \\ &\left.+\Re\left\{(\rho^t\tilde{\mathbf{H}}_k^t+(1-\rho^t)\mathbf{f}_k^t)^\dagger\left(\mathbf{w}-\mathbf{w}^t\right)\right\}\right) \\ &+\tau\left\|\mathbf{w}-\mathbf{w}^t\right\|^2,\end{aligned} \tag{16}$$

where $\mathbf{w}^t$ is the solution obtained in t-th iteration, constant $\tau>0$, $\{\rho^t\in(0,1]\}_{t=1}^{\infty}$ is a decreasing sequence about t,

$$\mathbf{H}_{u,k}^t = \mathrm{Bdiag}(\underbrace{\mathbf{h}_k^t\mathbf{h}_k^{t\dagger},\ldots,\mathbf{h}_k^t\mathbf{h}_k^{t\dagger}}_{K}), \tag{17a}$$

$$\mathbf{H}_{u/k}^t = \mathbf{H}_{u,k}^t - \mathrm{Bdiag}(\mathbf{0}_{N_b(k-1)},\mathbf{h}_k^t\mathbf{h}_k^{t\dagger},\mathbf{0}_{N_b(k-1)}), \tag{17b}$$

$$\tilde{\mathbf{H}}_k^t = -\frac{2\mathbf{H}_{u,k}^t\mathbf{w}^t}{\mathbf{w}^{t\dagger}\mathbf{H}_{u,k}^t\mathbf{w}^t+\sigma_k^2} + \frac{2\mathbf{H}_{u/k}^t\mathbf{w}^t}{\mathbf{w}^{t\dagger}\mathbf{H}_{u/k}^t\mathbf{w}^t+\sigma_k^2}, \tag{17c}$$

$\mathrm{Bdiag}(\mathbf{A}_1,\ldots,\mathbf{A}_K)$ denotes a block diagonal matrix with diagonal blocks $\mathbf{A}_1,\ldots,\mathbf{A}_K$, f_k^t and $\mathbf{f}_k^t$ are the approximation for the objective function and the gradient of the objective function, and they are updated recursively according to

$$\begin{aligned}f_k^t = &\left(1-\rho^t\right)f_k^{t-1}+\rho^t\left(\log(\mathbf{w}^{t\dagger}\mathbf{H}_{u/k}^t\mathbf{w}^t+\sigma_k^2)\right. \\ &\left.-\log(\mathbf{w}^{t\dagger}\mathbf{H}_{u,k}^t\mathbf{w}^t+\sigma_k^2)\right),\end{aligned} \tag{18a}$$

$$\mathbf{f}_k^t = \left(1-\rho^t\right)\mathbf{f}_k^{t-1}+\rho^t\tilde{\mathbf{H}}_k. \tag{18b}$$

Despite not containing slack variables, the surrogate function $g(\mathbf{w};\mathbf{w}^t)$ in (16) still conforms to the definition of structured surrogate function in [16].[1]

[1]By choosing the proper sequence $\{\rho^t\}_{t=1}^{\infty}$ and $\{\eta^t\}_{t=1}^{\infty}$ as shown in Appendix, we can verify that the surrogate function $g(\mathbf{w};\mathbf{w}^t)$ satisfies the assumptions 2 and 3 in [16]. Limited by space, the details are omitted.

Thus, in $(t+1)$-th iteration, we need to solve the following QCQP

$$\min_{\mathbf{w}} \quad g(\mathbf{w};\mathbf{w}^t) \tag{19a}$$
$$\text{s.t.} \quad (15b), (15c). \tag{19b}$$

Applying consensus-ADMM to solve problem (19), we need to solve the following subproblems iteratively,

$$\mathbf{w}^{s+1} \leftarrow \arg\min_{\mathbf{w}} g(\mathbf{w};\mathbf{w}^t) + \beta \sum_{i=1}^{2} \|\mathbf{x}_i^s - \mathbf{w} + \mathbf{v}_i^s\|^2, \tag{20a}$$

$$\mathbf{x}_i^{s+1} \leftarrow \arg\min_{\mathbf{x}_i} \ \|\mathbf{x}_i - \mathbf{w}^{s+1} + \mathbf{v}_i^s\|^2, \quad \text{s.t.} \begin{cases} \mathbb{E}\left[\text{MSE}(\mathbf{u},\mathbf{a},\mathbf{x}_i)\right] \le \xi, & \text{if } i=1, \\ \|\mathbf{x}_i\|^2 \le P_{\text{BS}}, & \text{if } i=2, \end{cases} \tag{20b}$$

$$\mathbf{v}_i^{s+1} \leftarrow \mathbf{x}_i^{s+1} - \mathbf{w}^{s+1} + \mathbf{v}_i^s, \tag{20c}$$

where auxiliary variables $\mathbf{w} = \mathbf{x}_i, i = 1,2$ are introduced to reformulate the problem (19) into the consensus form, $\mathbf{v}_i$ is the dual variable and $\beta \ge 0$ is the penalty parameter. Problem (20a) is an unconstraint convex problem, and the closed form solution is given as

$$\mathbf{w}^{s+1} = \frac{1}{\tau + 2\beta}\Big(\tau \mathbf{w}^t + \beta \textstyle\sum_{i=1}^{2}(\mathbf{x}_i^s + \mathbf{v}_i^s) + (1-\rho^t)\sum_{k=1}^{K}\mathbf{f}_k^{t-1} - \frac{\rho^t}{2}\sum_{k=1}^{K}\tilde{\mathbf{H}}_k^t\Big). \tag{21}$$

The semi-closed solution of problem (20b) is [15]

$$\mathbf{x}_i^{s+1} = \begin{cases} (\mathbf{I} + \mu_i \tilde{\mathbf{J}})^{-1}(\mathbf{w}^{s+1} - \mathbf{v}_i^s), & \text{if } i=1, \\ (1+\mu_i)^{-1}(\mathbf{w}^{s+1} - \mathbf{v}_i^s), & \text{if } i=2, \end{cases} \tag{22}$$

where $\tilde{\mathbf{J}} = \text{Bdiag}(\underbrace{\dot{\mathbf{J}},\ldots,\dot{\mathbf{J}}}_{K})$, $\dot{\mathbf{J}} = \alpha(\mathbf{u}^\dagger \mathbf{\Theta}_J \mathbf{u} \mathbf{\Psi}_J + \bar{\mathbf{J}}^\dagger \mathbf{u}\mathbf{u}^\dagger \bar{\mathbf{J}})$.

Denote $\mathbf{w}^\star$ as the solution of problem (20), and $\mathbf{w}^t$ is updated according to

$$\mathbf{w}^{t+1} = (1-\eta^t)\mathbf{w}^t + \eta^t \mathbf{w}^\star, \tag{23}$$

where $\{\eta^t \in (0,1]\}_{t=1}^{\infty}$ is a decreasing sequence about t.

C. Algorithm, Convergence, and Complexity

The proposed fast stochastic algorithm for solving the stochastic problem (7) is summarized in Algorithm 1.

Convergence: As the number of the iteration increases, Algorithm 1 converges. Please see Appendix for details.

Complexity: The computation burden of Algorithm 1 mainly comes from finding μ_l and μ_i by bisection method, which takes the complexity about $\mathcal{O}((LT_a + K^2 T_w)N_{BS}^2 + N_{BS}^3 K^3)$ [15], where T_a and T_w are the number of times that step 6 and step 17 are executed, respectively.

IV. Numerical Results

In this section, numerical results are conducted to evaluate the performance of the proposed fast stochastic algorithm in comparison with the CSSCA algorithm [16]. All channels are assumed to follow Rayleigh fading channel models, that is, the channel coefficients are modeled as i.i.d. circularly symmetric complex Gaussian random variables with zero mean and unit variance. If not specified, the number of antennas at the BS is $N_{BS} = 12$, the number of users is $K = 5$, the number of sensors is $L = 20$ [4], the MSE threshold is $\xi = 2$, the powers of noise are $\sigma^2 = 1$ and $\sigma_k^2 = \sigma^2 + 0.1\ LP_l$, the power budget at the BS and each sensor are $P_{\text{BS}}/\sigma^2 = 20$ dB and $P_l/\sigma^2 = 10$ dB [12], respectively, the covariance matrices $\mathbf{\Psi}_J$ and $\mathbf{\Theta}_J$ follow the definition in [12] with estimation error variance $\sigma_e^2 = 0.002$, passive loop-interference suppression $\alpha = 0.5$ [10]. All simulations are performed in MATLAB R2021b, and the CVX [17] are used to solve the SDPs. The simulation results are averaged over 100 randomly generated estimated CSI realizations.

Algorithm 1 The Proposed Fast Stochastic Algorithm

1: Initialize $\mathbf{a}$, $\mathbf{w}$, $\{\rho^t\}_{t=1}^{\infty}$ and $\{\eta^t\}_{t=1}^{\infty}$;
2: **repeat**
3: $n \leftarrow 0$;
4: **repeat**
5: Update $\mathbf{u}$ by (11);
6: Update a_l by (14), $l = 1,\ldots,L$;
7: $n \leftarrow n+1$;
8: **until** $\mathbf{u}$ and $\mathbf{a}$ are convergence;
9: $t \leftarrow 0$
10: $f_k^t \leftarrow 0, \mathbf{f}_k^t \leftarrow \mathbf{0}, k = 1,\ldots,K$;
11: **repeat**
12: Realize $\mathbf{h}_k^t, k = 1,\ldots,K$;
13: Construct $g(\mathbf{w};\mathbf{w}^t)$, $\mathbf{H}_{u,k}^t$ and $\mathbf{H}_{u/k}^t$ according to (16) and (17), $k = 1,\ldots,K$;
14: $s \leftarrow 0$;
15: **repeat**
16: Update $\mathbf{w}^{s+1}$ by (21);
17: Update $\mathbf{x}_i^{s+1}$ by (22), $i = 1,2$;
18: Update $\mathbf{v}_i^{s+1}$ by (20c), $i = 1,2$;
19: $s \leftarrow s+1$;
20: **until** $\mathbf{w}^s$ is convergence;
21: $\mathbf{w}^\star \leftarrow \mathbf{w}^s$;
22: Update f_k^t and $\mathbf{f}_k^t$ according to (18), $k = 1,\ldots,K$;
23: Update $\mathbf{w}^{t+1}$ according to (23);
24: $t \leftarrow t+1$;
25: **until** $\mathbf{w}^t$ is convergence;
26: **until** $\mathbf{u}$, $\mathbf{a}$ and $\mathbf{w}$ are convergence.

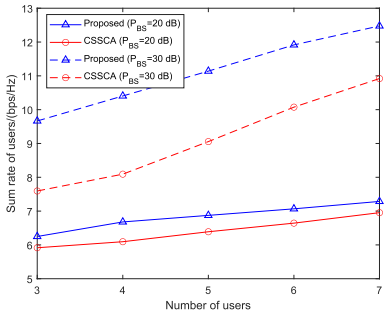

Fig. 1. The sum rate of users under different numbers of users.

In Fig. 1, we present the sum rate of users versus the numbers of users. It is observed that the sum rate of users increases as the number of users increases, and a higher transmit power budget of the BS leads to a higher sum rate. The proposed algorithm outperforms the CSSCA algorithm.

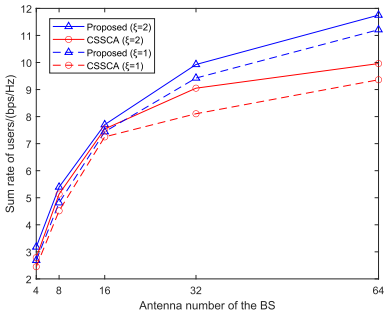

Fig. 2. The sum rate of users under different antenna numbers of the BS.

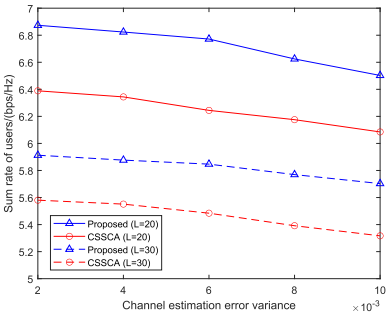

Fig. 3. The sum rate of users under different channel estimation error variances.

Additionally, the superiority of the proposed algorithm is more significant when the power budget at the BS increases.

In Fig. 2, we present the sum rate of users versus the antenna numbers of the BS. It can be observed that the sum rate of users increases as the antenna number of the BS increases. A lower MSE threshold results in a smaller feasible region, which leads to a lower sum rate. Furthermore, the proposed algorithm consistently outperforms the CSSCA algorithm. However, the sum rate of users will not increase indefinitely with the increase of the number of base station antennas. Since the noise of users and the interference caused by sensors do not tend to zero, and the limited transmitting power of the base station, the SINR of each user is limited.

In Fig. 3, we present the sum rate of users versus the channel estimation error variance. It can be observed that the sum rate of users decreases as the channel estimation error variance increases. The participation of more sensors results in higher interference power, which in turn diminishes the sum rate of users. Furthermore, the proposed algorithm achieves better performance than the CSSCA algorithm.

V. Conclusion

This letter investigates a full-duplex network that integrates communication and AirComp, considering the presence of imperfect CSI. Based on a new surrogate function, we have proposed a fast stochastic algorithm that jointly optimizes the power factor of sensors and the beamforming of BS to maximize the sum rate of users, and the closed or semi-closed form solution of each optimization variable has been derived. The effectiveness of the proposed algorithm has been demonstrated through numerical results.

Appendix
The Convergence Proof of Algorithm 1

The MSE has a lower bound since it is non-negative. Since the optimized $\mathbf{u}$ (or $\mathbf{a}$) in the current iteration is a feasible point in the next iteration, the value of objective function (10) (or (12a)) is non-increasing as the iterations process. Thus, the value of objective function (8a) is convergence.

Similarly, the value of objective function (15a) is non-decreasing as the iterations process (step 2 in Algorithm 1). The feasible region of problem (15) is compact and convex (satisfying the Slater condition), and the surrogate function (16) satisfies the definitions of the structured surrogate function [16]. Therefore, by choosing proper $\{\rho^t\}_{t=1}^{\infty}$ and $\{\eta^t\}_{t=1}^{\infty}$ satisfy that $\lim_{t\to\infty}\rho^t \to 0$, $\sum_{t=1}^{\infty}\rho^t \to \infty$, $\sum_{t=1}^{\infty}(\rho^t)^2 < \infty$, $\lim_{t\to\infty}\frac{\rho^t}{\eta^t} \to 0$, according to the Theorem 1 in [16], for any feasible initial point $\mathbf{w}^0$, $\{\mathbf{w}^t\}_{t=1}^{\infty}$ converges to a stationary point of problem (15).

From the above, the value of objective function (7a) is non-decreasing. Because the feasible region of problem (7) is finite and the objective function is continuous, Algorithm 1 converges.

References

[1] X. Chen et al., "Massive access for 5G and beyond," *IEEE J. Sel. Areas Commun.*, vol. 39, no. 3, pp. 615–637, Mar. 2021.

[2] S. Wang et al., "Integrated sensing, communication, and computation over-the-air: Beampattern design," in *Proc. IEEE Int. Conf. Commun. Workshops (ICC Workshops)*, Rome, Italy, May 2023, pp. 458–463.

[3] Q. Li et al., "Joint optimization of secure over-the-air computation and reliable multicasting assisted by a MIMO untrusted two-way relay," *IEEE Internet Things J.*, vol. 10, no. 19, pp. 17500–17514, Oct. 2023.

[4] Q. Qi et al., "Integrating sensing, computing, and communication in 6G wireless networks: Design and optimization," *IEEE Trans. Commun.*, vol. 70, no. 9, pp. 6212–6227, Sep. 2022.

[5] X. Li et al., "Integrated sensing, communication, and computation over-the-air: MIMO beamforming design," *IEEE Trans. Wireless Commun.*, vol. 22, no. 8, pp. 5383–5398, Aug. 2023.

[6] X. Li et al., "Wirelessly powered data aggregation for IoT via over-the-air function computation: Beamforming and power control," *IEEE Trans. Wireless Commun.*, vol. 18, no. 7, pp. 3437–3452, Jul. 2019.

[7] P. Chen, B. Lyu, H. Guo, and Z. Yang, "Sum computational bits maximization for full-duplex enabled wireless-powered mobile edge computing systems," in *Proc. IEEE/CIC Int. Conf. Commun. China (ICCC)*, Foshan, China, Aug. 2022, pp. 256–261.

[8] Z. He et al., "Full-duplex communication for ISAC: Joint beamforming and power optimization," *IEEE J. Sel. Areas Commun.*, vol. 41, no. 9, pp. 2920–2936, Sep. 2023.

[9] X. Shi and Z. Zhang, "Multi parameter trade-off of full duplex SWIPT bidirectional DF relay system for D2D communications," in *Proc. IEEE Int. Conf. Consum. Electron. Comput. Eng. (ICCECE)*, Guangzhou, China, Jan. 2021, pp. 676–682.

[10] C. Hu, Q. Li, Q. Zhang, and J. Qin, "Secure transceiver design and power control for over-the-air computation networks," *IEEE Commun. Lett.*, vol. 26, no. 7, pp. 1509–1513, Jul. 2022.

[11] P. Das and N. B. Mehta, "Rate-optimal relay selection for average interference-constrained underlay CR," *IEEE Trans. Commun.*, vol. 65, no. 12, pp. 5137–5148, Dec. 2017.

[12] C. Xing, S. Ma, and Y.-C. Wu, "Robust joint design of linear relay precoder and destination equalizer for dual-hop amplify-and-forward MIMO relay systems," *IEEE Trans. Signal Process.*, vol. 58, no. 4, pp. 2273–2283, Apr. 2010.

[13] Z. Lin et al., "Refracting RIS aided hybrid satellite-terrestrial relay networks: Joint beamforming design and optimization," *IEEE Trans. Aerosp. Electron. Syst.*, vol. 58, no. 4, pp. 3717–3724, Aug. 2022.

[14] Z. Lin et al., "Pain without gain: Destructive beamforming from a malicious RIS perspective in IoT networks," *IEEE Internet Things J.*, vol. 11, no. 5, pp. 7619–7629, Mar. 2024.

[15] K. Huang and N. Sidiropoulos, "Consensus-ADMM for general quadratically constrained quadratic programming," *IEEE Trans. Signal Process.*, vol. 64, no. 20, pp. 5297–5310, Oct. 2016.

[16] A. Liu, V. K. N. Lau, and B. Kananian, "Stochastic successive convex approximation for non-convex constrained stochastic optimization," *IEEE Trans. Signal Process.*, vol. 67, no. 16, pp. 4189–4203, Aug. 2019.

[17] M. Grant and S. Boyd. (2014). *CVX: MATLAB Software for Disciplined Convex Programming*. [Online]. Available: http://cvxr.com/cvx